

Eclipsing Binary Stars in the OGLE-III Galactic Disk Fields*

P. Pietrukowicz¹, P. Mróz¹, I. Soszyński¹,
 A. Udalski¹, R. Poleski^{1,2}, M. K. Szymański¹,
 M. Kubiak¹, G. Pietrzyński^{1,3}, Ł. Wyrzykowski^{1,4},
 K. Ulaczyk¹, S. Kozłowski¹ and J. Skowron¹

¹Warsaw University Observatory, Al. Ujazdowskie 4, 00-478 Warszawa, Poland
 e-mail: (pietruk,pmroz,soszynsk,udalski,rpoleski,msz,mk,pietrzyn,
 wyrzykow,kulaczyk,simkoz,jskowron)@astrouw.edu.pl

²Department of Astronomy, Ohio State University, 140 W. 18th Ave.,
 Columbus, OH 43210, USA

³Universidad de Concepción, Departamento de Física,
 Casilla 160-C, Concepción, Chile

⁴Institute of Astronomy, University of Cambridge, Madingley Road,
 Cambridge CB3 0HA, UK

ABSTRACT

We present the analysis of 11 589 eclipsing binary stars identified in twenty-one OGLE-III Galactic disk fields toward constellations of Carina, Centaurus, and Musca. All eclipsing binaries but 402 objects are new discoveries. The binaries have out-of-eclipse brightness between $I=12.5$ mag and $I=21$ mag. The completeness of the catalog is estimated at a level of about 75%. Comparison of the orbital period distribution for the OGLE-III disk binaries with systems detected in other recent large-scale Galactic surveys shows the maximum around 0.40 d and an almost flat distribution between 0.5 d and 2.5 d, independent of population. Ten doubly eclipsing systems and one eclipsing-ellipsoidal object were found among thousands of variables. Nine of them are candidates for quadruple systems. We also identify ten eclipsing subdwarf-B type binary stars and numerous eclipsing RS CVn type variables. All objects reported in this paper are part of the OGLE-III Catalog of Variable Stars.

Galaxy: disk – binaries: eclipsing – variables: general – starspots

1 Introduction

Binaries are common among stars of our universe. It is believed that two out of every three stars in our Galaxy are in a binary or a multiple system and a few per cent of main sequence binaries could be observed as eclipsing systems (Söderhjelm and Dischler 2005). Eclipsing binaries are a powerful tool in astrophysical diagnostics. They are widely used as probes of stellar structure and evolution. Eclipsing systems allow a direct determination of the fundamental parameters (such as masses and radii) of the component stars to high accuracy (*e.g.*, Pietrzyński *et al.* 2010, 2012) and provide excellent tests of stellar models (*e.g.*, Ribas *et al.* 2000, Morales *et al.* 2010). Binaries serve as superb distance indicators to nearby galaxies (*e.g.*, Bonanos *et al.* 2006, North *et al.* 2010, Vildardell *et al.* 2010, Pietrzyński *et al.* 2013) and help to trace the structure and evolution of the Milky Way (*e.g.*, Nataf *et al.* 2012, Hełminiak *et al.* 2013). Precise measurements of orbital motion of a binary can be used to search for orbiting companions through the light-travel time effect and transits (*e.g.*, Doyle *et al.* 2011, Welsh *et al.* 2012).

*Based on observations obtained with the 1.3-m Warsaw telescope at the Las Campanas Observatory of the Carnegie Institution for Science.

Following the advent of wide-field photometric surveys, the number of new eclipsing variables has increased rapidly. The Optical Gravitational Lensing Experiment (OGLE) is a long-term project with the main aim to detect microlensing events toward the Galactic bulge (Udalski *et al.* 1993, Udalski 2003). However, regular observations of the Milky Way and Magellanic Cloud stars, conducted in some fields for over 21 years, allow us to discover and explore the variety of variable objects. The OGLE collection of classified variable stars recently has exceeded 400 000 objects. Most of them are pulsating red giants such as Long Period Variables (~ 340000 objects, *e.g.*, Soszyński *et al.* 2013), Classical Cepheids (~ 8000 objects, *e.g.*, Soszyński *et al.* 2008), and RR Lyrae stars (~ 45000 , objects, *e.g.*, Soszyński *et al.* 2011). Among binary stars, a large sample of eclipsing systems (~ 26000) was found in the Large Magellanic Cloud (Graczyk *et al.* 2011).

This paper presents a catalog of 11 589 eclipsing stars detected in twenty-one fields located in the Galactic disk toward constellations of Carina, Centaurus, and Musca. The presented sample is a part of the OGLE-III Catalog of Variable Stars. In the following sections of this paper, we describe: the observations and reductions (Section 2), the completeness of the search (Section 3), the catalog itself (Section 4), likely X-ray counterparts to the optical detections (Section 5), the brightness, amplitude, and period distributions (Section 6). In Section 7, we focus on selected interesting objects and finally, in Section 8, we summarize our results.

2 Observations and Data Reductions

All the data presented in this paper were collected with the 1.3-m Warsaw telescope at Las Campanas Observatory, Chile. The observatory is operated by the Carnegie Institution for Science. During the OGLE-III project, conducted in years 2001–2009, the telescope was equipped with an eight-chip CCD mosaic camera with a scale of 0.26 arcsec/pixel and a field of view of $35' \times 35'$. Details of the instrumentation setup can be found in Udalski (2003).

Twenty-one fields covering the total area of 7.12 deg² around the Galactic plane between longitudes $+288^\circ$ and $+308^\circ$ were observed. Their location in the sky is shown in Fig. 1. The time coverage as well as the number of data points obtained by the OGLE project varies considerably from field to field (Fig. 2 and Table 1). The vast majority of the observations, typically of 1500 to 2700 points per field, were collected through the *I*-band filter with exposure times of 120 s and 180 s. Additional observations, consisting of only 3–8 measurements, were carried out in the *V*-band filter with an exposure time of 240 s. Both filters closely resemble those of the standard Johnson-Cousins system.

The time-series photometry was obtained with the standard OGLE data reduction pipeline (Udalski *et al.* 2008, based on the Difference Image Analysis: DIA, Alard and Lupton 1998, Woźniak 2000). A period search was performed using the FNPEAKS code (written by Z. Kołaczowski, private communication) for about 8.8×10^6 stars containing at least 30 points in the *I*-band light curve. About 345 500 detections with a signal to noise $S/N > 10$ were visually checked for any kind of variability. The search resulted in about 13 000 eclipsing binary candidates, ≈ 1000 ellipsoidal-like candidates, ≈ 1000 pulsating star candidates, and $\approx 15 000$ miscellaneous variables (mostly stars with spots). Details on the detected dwarf novae are presented in Mróz *et al.* (2013), while papers on other variables (in particular on the pulsating stars) are in preparation.

Table 1: Basic data on monitored Galactic disk fields in OGLE-III

Field	l	b	N_{nights}	$N_{\text{exp},I}$
CAR100	290°6544	-0°7510	202	2698
CAR104	289°8439	-1°7249	161	1641
CAR105	289°2911	-1°9906	167	1770
CAR106	290°5054	-1°6063	47	896
CAR107	288°9089	-2°5647	135	1530
CAR108	288°6343	-2°0343	135	1513
CAR109*	288°4607	-2°9904	145	1811
CAR110	288°1846	-2°4606	135	1475
CAR111	288°3599	-1°5037	134	1697
CAR112	289°0276	-1°4562	134	1688
CAR113	289°5717	-1°1922	134	1676
CAR114	289°3178	-0°6516	134	1672
CAR115*	288°2783	-3°0629	234	2001
CAR116	288°2176	-3°7841	233	1963
CAR117	288°7274	-3°5017	232	1922
CAR118	288°6602	-4°2207	230	1888
CEN106	293°4598	+0°5784	44	819
CEN107	296°2458	+0°1238	44	815
CEN108	307°4281	-1°7417	278	2374
MUS100	305°4335	-2°0928	279	2468
MUS101	306°4749	-2°3261	280	2428

* – Fields CAR109 and CAR115 significantly overlap with each other in the sky, but have no common nights.

In the next step, we rejected from the list of eclipsing binary candidates false detections and artifacts that mimicked variability of neighboring real eclipsing stars. Then, we manually removed outlying points from the light curves of all eclipsing stars and improved orbital periods of binaries with $P > 1.0$ d. The uncertainty of the period is estimated at a level of about $10^{-5}P$ for $P > 1.0$ d. For stars with $P < 1.0$ d their periods together with errors were improved using the TATRY code (Schwarzenberg-Czerny 1996). After the period correction we re-examined the list for the remaining false period detections and for common variables independently detected in overlapping fields. Combined light curves containing more data points allowed us to additionally improve the orbital periods of the common stars. We note that we were not able to estimate the orbital period for 27 binaries with very small number of eclipses.

In the last reduction step, each variable was calibrated from the instrumental to the standard magnitudes. For stars with available measurements in the V band we evaluated $V - I$ colors around corresponding phases in the I -band light curve. Then the mean color was calculated after rejection of two most outlying values. In the case of red stars ($V - I > 1.5$ mag) the I -band photometry had to be additionally corrected according to formula presented in Szymański *et al.* (2011). For eclipsing variables without any measurement in V (*i.e.*, mostly faint objects with $I > 19$ mag) the $V - I$ value in the color term of the transformation was derived from a linear extrapolation of the $V - I$ vs. I relation for stars with $17 < I < 19$ mag in the same subfield.

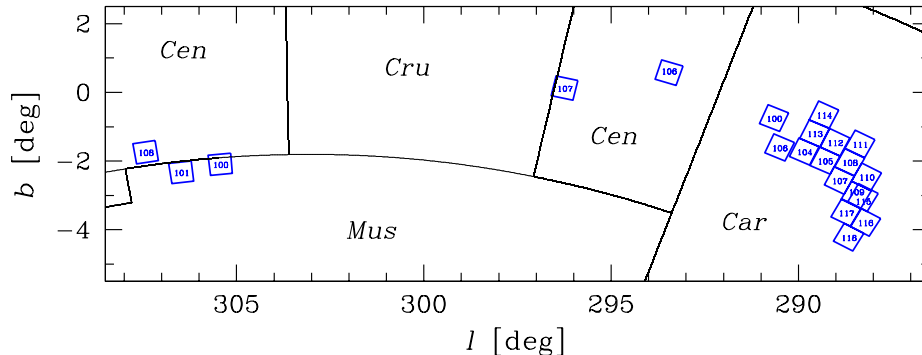


Fig. 1. Location of the twenty-one OGLE-III disk fields in the Galactic coordinates. Each field covers $35' \times 35'$ in the sky. Two fields, CAR109 and CAR115, overlap with each other in $\approx 67\%$. The total monitored area is 7.12 deg^2 .

3 Completeness of the Search

While preparing the final list of eclipsing binaries we searched for the same variables detected in overlapping regions. Within the largest overlapping region between fields CAR109 and CAR115 we found 206 common stars out of a total of 308 eclipsing variables detected in this area. This gives an upper limit for the completeness of the sample of $2x/(x+1) \approx 80\%$, where $x = 206/308$. However, a more realistic estimate of the completeness of our search is based on a comparison with an independent variability survey.

For four contiguous nights in April 2005 a 0.052 deg^2 area located within the OGLE-III disk field CAR105 was monitored to follow-up selected OGLE transiting candidates (Udalski *et al.* 2002abc, 2003). A dataset consisting of 660 V -band images was taken with VIMOS of the European Southern Observatory 8.2-m Very Large Telescope (VLT). Of nine OGLE transits in the VIMOS area, two objects were later confirmed to be caused by planets: OGLE-TR-111b (Pont *et al.* 2004) and OGLE-TR-113b (Bouchy *et al.* 2004, Konacki *et al.* 2004). A search for variables brought 348 objects among 50 897 stars in the brightness range between $V=15.4 \text{ mag}$ and $V=24.5 \text{ mag}$ (Pietrukowicz *et al.* 2009). Despite different bands used in the OGLE and VIMOS surveys, the depth is very similar or even slightly shallower in the case of OGLE. Both surveys are very complementary. While VIMOS observations have an excellent sampling of ≈ 165 exposures per night, OGLE collected about 1800 points in 167 nights over four seasons. We cross-matched the list of VIMOS variables with the list of OGLE eclipsing stars. Eighty-nine objects were common, 23 OGLE variables were not found in the VIMOS list, while 38 VIMOS eclipsing binaries were not detected during the OGLE search. Based on these numbers we conclude that the completeness of the catalog of eclipsing binaries is $(89 + 23)/(89 + 23 + 38) \approx 75\%$. Thirty-four of the missing VIMOS binaries were added to our list.

The final list of eclipsing variables was additionally extended by 139 OGLE transits detected in the beginning of the third phase of the project and reported in Udalski *et al.* (2002abc, 2003, 2008) and Pont *et al.* (2008). Out of a total number of 155 transit candidates reported in the Galactic disk five transits were spectroscopically confirmed as being due to planets: OGLE-TR-111b (Pont *et al.* 2004), OGLE-TR-113b (Bouchy *et al.* 2004, Konacki *et al.* 2004), OGLE-TR-

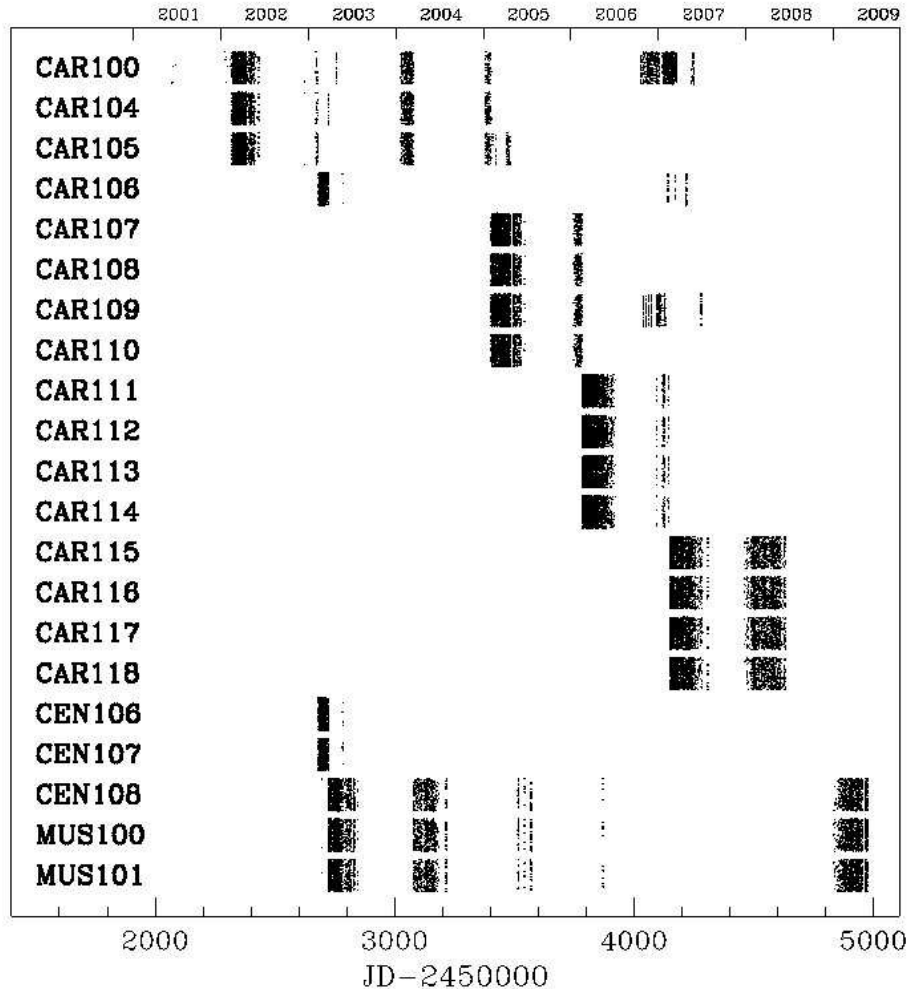


Fig. 2. Graphical log of observations of the OGLE-III disk fields. Each single point represents one exposure. To show irregular coverage of the observations for each field we randomly spread the points in the vertical direction. The number of points is between 815 and 2698 per field.

132b (Bouchy *et al.* 2004), OGLE-TR-182b (Pont *et al.* 2008), and OGLE-TR-211b (Udalski *et al.* 2008). The remaining stars but five objects turned out to be either binary systems, multiple systems or systems with unverified planetary companions. Six of the systems were independently found in our variability search. With the longer database we have improved the orbital periods for most of the 145 OGLE transit objects.

4 The Catalog of Eclipsing Binaries in the OGLE-III Disk Fields

The OGLE-III catalog of eclipsing binaries in the Galactic disk, containing tables with basic parameters, time-series *I*- and *V*-band photometry, and finding charts, is available to the astronomical community from the OGLE Internet

Archive:

http://ogle.astroww.edu.pl
ftp://ftp.astroww.edu.pl/ogle/ogle3/OIII-CVS/gd/ecl/

Eclipsing variables in the Galactic disk are arranged according to increasing right ascension and named as OGLE-GD-ECL-NNNNN, where NNNNN is a five-digit consecutive number. Besides coordinates of the binaries, their orbital periods, and period uncertainties, we also provide information on the maximum brightness in I , the I -band amplitude, the $V - I$ color, the moment of the primary minimum, classification to contact or non-contact type, and a cross-match identification name with the VIMOS survey (Pietrukowicz *et al.* 2009, 2012) and the list of OGLE-II eclipsing binaries in Carina (Huemmerich and Bernhard 2012), if exists.

5 X-ray counterparts

Close binaries are often chromospherically active systems, hence they can emit intense coronal X-ray radiation. In the optical range, the characteristic features of such systems are sporadic flares observed over timescales of minutes (*e.g.*, Osten *et al.* 2012) and relatively large variations in the out-of-eclipse brightness ($\lesssim 0.5$ mag) attributed to spot activity (*e.g.*, Udalski *et al.* 2012, Taş *et al.* 2013, Rozycka *et al.* 2013).

We conducted a search for eclipsing binary counterparts to 220 X-ray sources located within the OGLE-III Galactic disk area with the help of the XAMIN system of the High Energy Astrophysics Science Archive Research Center[†]. The sources were detected by diverse satellite X-ray observatories and of different angular resolution: Chandra ($\sigma_d=0''.6$ at 90% uncertainty circle), XMM-Newton ($1''.5$ for bright and $2''-4''$ for faint sources), and ROSAT ($\sim 6''$). We searched for optically variable counterparts within a radius of $18''.2$ (corresponding to 70 pix of the OGLE-III camera) around the X-ray sources. Two Chandra X-ray sources, X104523.77-603051.7 and X110523.68-610822.2, coincide with relatively bright eclipsing binaries OGLE-GD-ECL-02102 ($I_{max}=14.23$ mag) and OGLE-GD-ECL-06924 ($I_{max}=13.71$ mag), respectively. The angular distance in the sky between the coincided optical and X-ray positions is only $0''.78$ and $0''.23$, respectively. Moreover, large variations observed in the light curve of OGLE-GD-ECL-06924 (shown in Fig. 12 in Section 7.4) is a strong evidence for the ideal X-ray-optical cross-match in this case. One XMM-Newton source, J104704.2-620158, located $5''.1$ from OGLE-GD-ECL-02579 and two ROSAT sources, J1105.0-6116 and J1155.4-6211, located $3''.6$ from OGLE-GD-ECL-06854 and $5''.0$ from OGLE-GD-ECL-08457, respectively, are counterpart candidates for these eclipsing systems. For another two ROSAT X-ray sources (J1105.7-6054 and J115219.1-615605) we found nearby eclipsing variables (OGLE-GD-ECL-06974 and OGLE-GD-ECL-08046, respectively). However, the distances between the optical and X-ray positions of $2.05\sigma_d$ and $2.78\sigma_d$, respectively, make the cross-identification less certain.

[†]<http://heasarc.gsfc.nasa.gov/>

6 Brightness, Amplitude, and Period Distributions

In Fig. 3, we present the observed out-of-eclipse I -band brightness distribution for all binary stars found in the OGLE-III disk area. For stars with $I > 18$ mag the completeness of the sample drops significantly. Fig. 4 shows the I -band amplitude distributions for all detected eclipsing variables and variables brighter than $I = 18$ mag. From this plot we can infer that the sample of stars with $I < 18$ mag lacks systems with amplitudes < 0.2 mag.

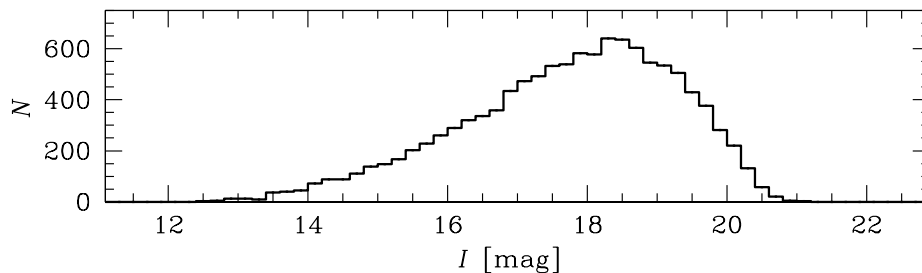


Fig. 3. Brightness distribution in the I band for 11 589 eclipsing variables detected in the OGLE-III Galactic disk fields. The bin size is 0.2 mag.

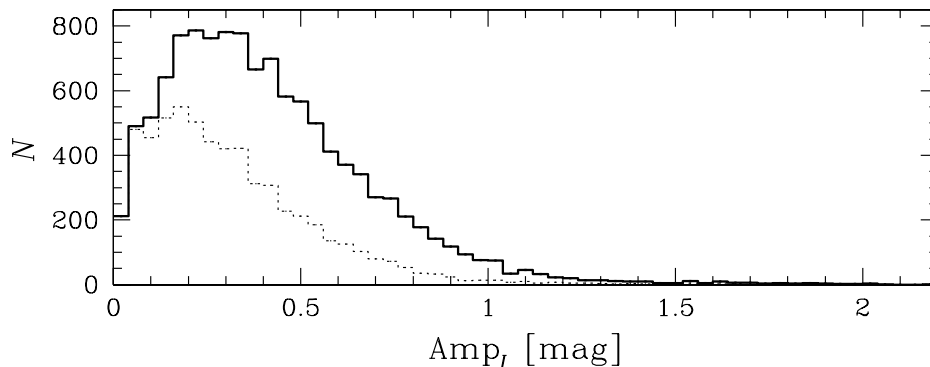


Fig. 4. Amplitude distributions for all 11 589 OGLE-III disk eclipsing variables (thick solid line) and 6023 variables with $I < 18$ mag (dotted line). The bin size is 0.04 mag.

In the next figure, Fig. 5, we plot the distribution of the orbital period for the OGLE-III disk binaries. The shortest orbital period of 0.07753698(1) d was found in a hot subdwarf binary star OGLE-GD-ECL-10384, while the longest orbital period of 103.502(1) d was measured for system OGLE-GD-ECL-03367. Based on the shape of the light curves we divided our whole sample into likely contact and non-contact systems. Contact systems constitute about 64% of all detected binaries. Period distributions for the two separate groups are also shown in Fig. 5. It is noticeable that the majority of binaries with $P < 0.5$ d are in contact. Among binaries with orbital periods around 0.7 d about half are contact systems. Their number significantly decreases around $P \approx 1.5$ d, although some of them may have longer periods. The shortest orbital period of a binary, classified as a probable contact system, equals to 0.1571319(2) d in

the case of OGLE-GD-ECL-00665, while the longest period of 19.6464(2) d was found in a contact system candidate OGLE-GD-ECL-03668. We have to stress that our classification is tentative. Contact system candidates with unusually short and unusually long periods are not confirmed and require more studies.

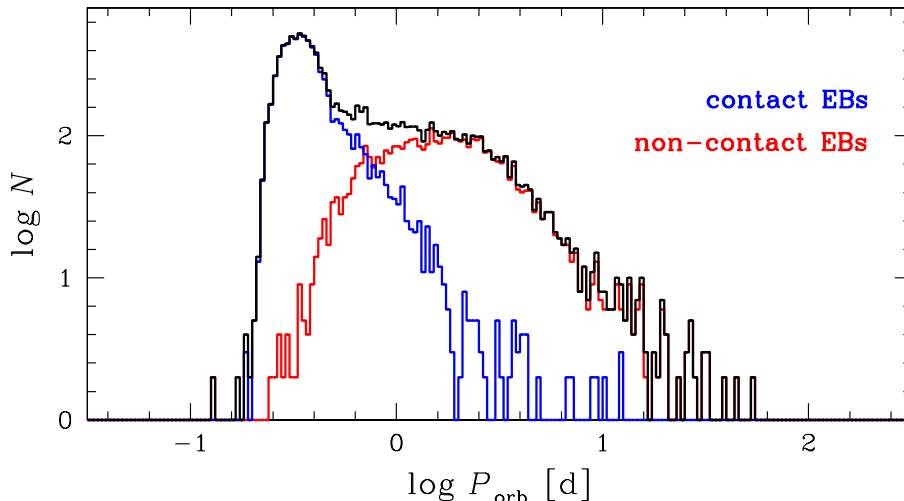


Fig. 5. Orbital period distribution for 11 562 OGLE-III disk eclipsing binaries (EBs) with a division into contact and non-contact systems. Note that the histogram shows the logarithm of the counts, thus bins with a single star appear blank.

The orbital period distribution for 6023 OGLE-III disk binaries with brightness $I < 18$ mag is shown in Fig. 6. In the same figure, we also draw the orbital period distributions for eclipsing binaries discovered in the course of two recent wide-field surveys: the All Sky Automated Survey (ASAS, Paczyński et al. 2006) and the Kepler space telescope (Slawson et al. 2011). The ASAS survey monitored stars with brightness $V \lesssim 14$ mag and declination $< +28^\circ$ for 5–8 years (Pojmański 1997, 2002, 2003). The presented period distribution is based on 5462 ASAS variables unambiguously classified as eclipsing binaries with $V < 12$ mag. The Kepler telescope monitored a fixed area of 115 deg^2 toward mainly constellations of Cygnus and Lyra between Galactic latitudes $+6^\circ$ and $+23^\circ$ in searches for transiting extrasolar planets (*e.g.*, Koch *et al.* 2010). The plotted orbital period distribution is based on 1032 binaries with Kepler magnitudes < 14 mag which were identified in a dataset of continuous observations lasting 125 days.

Although the three surveys, OGLE, ASAS, and Kepler, observed different Galactic regions and different stellar populations, we can draw common conclusions from the comparison presented in Fig. 6. First, the distribution of the orbital period peaks around 0.40 d. Obviously, this maximum refers to contact binaries. Second, for orbital periods between 0.5 d and 2.5 d the distribution is either flat or decreases very weakly with P . Linear fit to the rich OGLE data in this regime does not give us a clear answer: $\log N \propto (-0.025 \pm 0.036)\log P$. For periods longer than 2.5 days the Kepler observations indicate a higher occurrence rate of binaries than more numerous and longer-duration ground-based observations from OGLE and ASAS. This period regime requires more data.

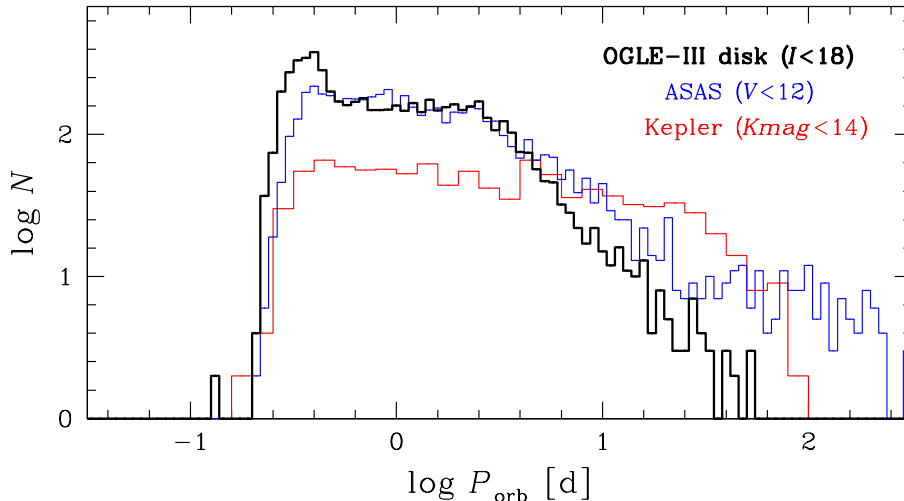


Fig. 6. Orbital period distribution for bright eclipsing binaries from the OGLE-III disk fields in comparison with results from the All-Sky Automatic Survey and the Kepler orbiting telescope.

7 Interesting Objects

7.1 Candidates for Double Binaries

Eleven single detections showing light variations due to the presence of two binary systems were found among thousands of eclipsing objects discovered in the OGLE-III disk fields. We subtracted the stronger component with the period P_a from each of the eleven light curves using Fourier series and searched for the second period P_b . By subtracting the light variations with P_b from the original light curve we improved the value of P_a . Resolved light curves are plotted in Figs. 7–9.

We made an attempt to verify photometrically if the double binaries either are likely blended objects observed almost exactly in the same line of sight or may form physically bound systems. In order to check that we measured centroid positions of these objects on images with the help of the DOPHOT software (Schechter, Saha and Mateo 1993). Then, separately in x and y directions, we phased the offsets from the mean position with periods P_a and P_b . The results are also included in Figs. 7–9, where we binned the measured offsets in $0.01P$ bins. One can notice that the position changes in OGLE-GD-ECL-00259b and OGLE-GD-ECL-04406a are correlated with the component’s light curves. This may indicate that nine of the observed double binaries (OGLE-GD-ECL-03436, 05310, 05390, 05656, 07057, 07157, 07443, 10263, 11021) are physically bound quadruple systems, while in the case of OGLE-GD-ECL-00259 and OGLE-GD-ECL-04406 the component binaries seem to be located almost along the same line of sight by pure chance.

The probability of such a chance position of two binaries is very small. The number of 11 589 binary stars detected over the whole OGLE-III disk area of 7.12 deg^2 gives on average 0.000126 objects per 1.0 arcsec^2 . At a separation of the mean seeing of the I -band images of $1''.2$ (Szymański *et al.* 2011) the expected number of eclipsing objects would be 0.00018 .

7.2 Subdwarf-B Type Binaries

In our search for binaries in the disk data we identified ten binaries with hot components manifesting their presence in the reflection effect and huge difference in depth of the two minima (see light curves in Fig. 10). The binaries have periods between 0.0775 d and 0.5066 d and five of them are the shortest period systems detected in the whole sample. These stars are very likely subdwarf B type (sdB) binaries.

7.3 Eclipsing RS CVn Type Stars

RS CVn variable stars are close binaries with active chromospheres. It is believed that brightness variations $\lesssim 0.5$ mag observed in this type of stars are caused by huge cool spots on the surface of the components. The high activity of the system reveals also in sporadic flares and X-ray radiation. In some systems, signs of accretion are seen (*e.g.*, Rozyczka *et al.* 2013, Kang *et al.* 2013). The presence of eclipses in a RS CVn type star helps to investigate the relation between its activity and the evolutionary stage of the binary. In Fig. 11, we present the best examples of RS CVn type stars identified in the OGLE sample. As we mentioned in Section 5, one of the presented systems, OGLE-GD-ECL-06924, has an X-ray counterpart.

7.4 Eclipsing Objects of Unknown Nature

In Fig. 12, we present phased light curves of three eclipsing variables whose nature is unknown. The objects have amplitudes between 0.13 mag and 0.27 mag in the I band and the observed $V - I$ color in the range from 2.97 mag to 3.38 mag. The asymmetric eclipse in OGLE-GD-ECL-03166 may indicate the presence of an accretion disk. Object OGLE-GD-ECL-06674 has a very short period of 0.13004370(7) d, typical for close compact binaries such as polars and intermediate polars. Unfortunately, there are no detected X-ray counterparts to these stars, what could help in their final identification.

8 Summary and conclusions

In this paper we report the identification of 11 589 eclipsing objects detected in the OGLE-III Galactic disk fields. All objects but 402 variable stars are new discoveries. The completeness of our catalog we estimate to be at a level of 75%. We tentatively classified the eclipsing stars into contact and non-contact systems. The first group constitutes about two-thirds of all identified systems. The orbital period distribution of the OGLE binaries shows a maximum at ≈ 0.40 d and an almost flat part between 0.5 d and 2.5 d. After comparison with results from the ASAS and Kepler data, we find that these two properties seem to be independent of population. A conclusion from the obtained period distribution is that binaries tend to shrink their orbits. This is in agreement with the well known fact of the mass and momentum loss during the evolution of binaries.

In Fig. 13, we plot an interesting finding based on our data: the ratio of non-contact to contact systems for latitudes $b < -1.5^\circ$ seems to be constant around 0.5, while it increases up to 1.0 around $b \sim -1.0^\circ$. This means that close to the Galactic plane there is a deficiency of systems in contact. There is a possibility

that some of the missing systems could have merged, as it was observed in the case of the red nova V1309 Sco (Tyłenda *et al.* 2011).

Eleven single unresolved detections showing light variations due to the presence of two binary systems were found among thousands of eclipsing objects. Astrometric analysis indicates that nine of the objects are good candidates for quadruple systems, while the other two are likely unresolved blends of two unbound binary systems. Our search for eclipsing objects brought identification of ten subdwarf-B type binaries and dozens of RS CVn type variables. We also found three objects with eclipses of unknown origin. All these objects need multi-band and spectroscopic follow-up studies.

Acknowledgments. This work has been supported by the Polish National Science Centre grant No. DEC-2011/03/B/ST9/02573 and the Polish Ministry of Sciences and Higher Education grant No. IP2012 005672 under Iuventus Plus programme. The OGLE project has received funding from the European Research Council under the European Community's Seventh Framework Programme (FP7/2007-2013)/ERC grant agreement No. 246678 to A.U.

REFERENCES

- Alard, C., and Lupton, R. H. 1998, *Astrophys. J.*, **503**, 325.
 Bonanos, A. Z., *et al.* 2006, *Astrophys. J.*, **652**, 313.
 Bouchy, F., Pont, F., Santos, N. C., Melo, C., Mayor, M., Queloz, D., Udry, S. 2004, *Astron. Astrophys.*, **421**, L13.
 Doyle, L. R., *et al.* 2011, *Science*, **333**, 1602.
 Graczyk, D., Soszyński, I., Poleski, R., Pietrzyński, G., Udalski, A., Szymański, M. K., Kubiak, M., Wyrzykowski, L., and Ulaczyk, K. 2011, *Acta Astron.*, **61**, 103.
 Huemmerich, S., and Bernhard, K. 2012, *Peremennye Zvezdy Prilozhenie*, **12**, 11.
 Helminiak, K. G., Devor, J., Minniti, D., and Sybilski, P. 2013, *MNRAS*, **432**, 2895.
 Kang, Y.-W., Yushchenko, A. V., Hong, K., Guinan, E. F., and Gopka, V. F. 2013, *Astron. J.*, **145**, 167.
 Koch, D. G. *et al.* 2010, *Astrophys. J.*, **713**, L79.
 Konacki, M., Torres, G., Sasselov, D. D., Pietrzyński, G., Udalski, A., Jha, S., Ruíz, M. T., Gieren, W., Minniti, D. 2004, *Astrophys. J.*, **609**, L37.
 Morales, J. C., Gallardo, J., Ribas, I., Jordi, C., Baraffe, I., and Chabrier, G. 2010, *Astrophys. J.*, **718**, 502.
 Mróz, P., Pietrukowicz, P., Soszyński, I., Udalski, A., Poleski, R., Szymański, M. K., Kubiak, M., Pietrzyński, G., Wyrzykowski, L., Ulaczyk, K., Kozłowski, S., and Skowron, J. 2013, *Acta Astron.*, **63**, NNN.
 Nataf, D. M., Gould, A., and Pinsonneault, M. H. 2012, *Acta Astron.*, **62**, 33.
 North, P., Gauderon, R., Barblan, F., and Royer, F. 2010, *Astron. Astrophys.*, **520A**, 74.
 Osten, R. A., Kowalski, A., Sahu, K., and Hawley, S. L. 2012, *Astrophys. J.*, **754**, 4.
 Paczyński, B., Szczygieł, D. M., Pilecki, B., and Pojmański, G. 2006, *MNRAS*, **368**, 1311.
 Pietrukowicz, P., Minniti, D., Fernández, J. M., Pietrzyński, G., Ruíz, M. T., Gieren, W., Díaz, R. F., Zoccali, M., and Hempel, M. 2009, *Astron. Astrophys.*, **503**, 651.
 Pietrukowicz, P., Minniti, D., Alonso-García, J., and Hempel, M. 2012, *Astron. Astrophys.*, **537**, A116.
 Pietrzyński, G. *et al.* 2010, *Nature*, **468**, 542.
 Pietrzyński, G. *et al.* 2012, *Nature*, **484**, 75.
 Pietrzyński, G. *et al.* 2013, *Nature*, **495**, 76.
 Pojmański, G. 1997, *Acta Astron.*, **47**, 467.
 Pojmański, G. 2002, *Acta Astron.*, **52**, 397.
 Pojmański, G. 2003, *Acta Astron.*, **53**, 341.
 Pont, F., Bouchy, F., Queloz, D., Santos, N. C., Melo, C., Mayor, M., Udry, S. 2004, *Astron. Astrophys.*, **426**, L15.
 Pont, F. *et al.* 2008, *Astron. Astrophys.*, **487**, 749.
 Ribas, I., Jordi, C., and Giménez, Á. 2000, *MNRAS*, **318**, L55.
 Rozyczka, M., Pietrukowicz, P., Kaluzny, J., Pych, W., Angeloni, R., Dèkány, I. 2013, *MNRAS*, **429**, 1840.
 Schechter, P. L., Saha, K., and Mateo, M. 1993, *P.A.S.P.*, **105**, 1342.

- Schwarzenberg-Czerny, A. 1996, *Astrophys. J.*, **460**, L107.
- Slawson, R. W., Prša, A., Welsh, W. F., Orosz, J. A., Rucker, M., Batalha, N. *et al.* 2011, *Astron. J.*, **142**, 160.
- Soszyński, I., Poleski, R., Udalski, A., Szymański, M. K., Kubiak, M., Pietrzyński, G., Wyrzykowski, L., Szewczyk, O., and Ulaczyk, K. 2008, *Acta Astron.*, **58**, 163.
- Soszyński, I., Dziembowski, W. A., Udalski, A., Poleski, R., Szymański, M. K., Kubiak, M., Pietrzyński, G., Wyrzykowski, L., Ulaczyk, K., Kozłowski, S., and Pietrukowicz, P. 2011, *Acta Astron.*, **61**, 1.
- Soszyński, I., Udalski, A., Szymański, M. K., Kubiak, M., Pietrzyński, G., Wyrzykowski, L., Ulaczyk, K., Poleski, R., Kozłowski, S., Pietrukowicz, P., and Skowron, J. 2013, *Acta Astron.*, **63**, 21.
- Söderhjelm, S. and Dischler, J. 2005, *Astron. Astrophys.*, **442**, 1003.
- Szymański, M. K., Udalski, A., Soszyński, I., Kubiak, M., Pietrzyński, G., Poleski, R., Wyrzykowski, L., and Ulaczyk, K. 2010, *Acta Astron.*, **60**, 295.
- Szymański, M. K., Udalski, A., Soszyński, I., Kubiak, M., Pietrzyński, G., Poleski, R., Wyrzykowski, L., and Ulaczyk, K. 2011, *Acta Astron.*, **61**, 83.
- Taş, G., and Evren, S. 2013, *Astr. Nachr.*, **334**, 251.
- Tylenda, R., Hajduk, M., Kamiński, T., Udalski, A., Soszyński, I., Szymański, M. K., Kubiak, M., Pietrzyński, G., Poleski, R., Wyrzykowski, L., and Ulaczyk, K. 2011, *Astron. Astrophys.*, **528A**, 114.
- Udalski, A., Szymański, M., Kaluzny, J., Kubiak, M., Krzemiński, W., Mateo, M., Preston, G. W., Paczyński, B. 1993, *Acta Astron.*, **43**, 289.
- Udalski, A., Paczyński, B., Żebruń, K., Szymański, M., Kubiak, M., Soszyński, I., Szewczyk, O., Wyrzykowski, L., and Pietrzyński, G. 2002a, *Acta Astron.*, **52**, 1.
- Udalski, A., Żebruń, K., Szymański, M., Kubiak, M., Soszyński, I., Szewczyk, O., Wyrzykowski, L., Pietrzyński, G. 2002b, *Acta Astron.*, **52**, 115.
- Udalski, A., Szewczyk, O., Żebruń, K., Pietrzyński, G., Szymański, M., Kubiak, M., Soszynski, I., and Wyrzykowski, L. 2002c, *Acta Astron.*, **52**, 317.
- Udalski, A., Pietrzyński, G., Szymański, M., Kubiak, M., Żebruń, K., Soszyński, I., Szewczyk, O., and Wyrzykowski, L. 2003, *Acta Astron.*, **53**, 133.
- Udalski, A. 2003, *Acta Astron.*, **53**, 291.
- Udalski, A. *et al.* 2008, *Astron. Astrophys.*, **482**, 299.
- Udalski, A., Szymański, M. K., Soszyński, I., and Poleski, R. 2008, *Acta Astron.*, **58**, 69.
- Udalski, A., Kowalczyk, K., Soszyński, I., Poleski, R., Szymański, M. K., Kubiak, M., Pietrzyński, G., Kozłowski, S., Pietrukowicz, P., Ulaczyk, K., Skowron, J., Wyrzykowski, L. 2012, *Acta Astron.*, **62**, 133.
- Vilardell, F., Ribas, I., Jordi, C., Fitzpatrick, E. L., and Guinan, E. F. 2010, *Astron. Astrophys.*, **509A**, 70.
- Welsh, W. F., *et al.* 2012, *Nature*, **481**, 475.
- Woźniak, P. R. 2000, *Acta Astron.*, **50**, 421.

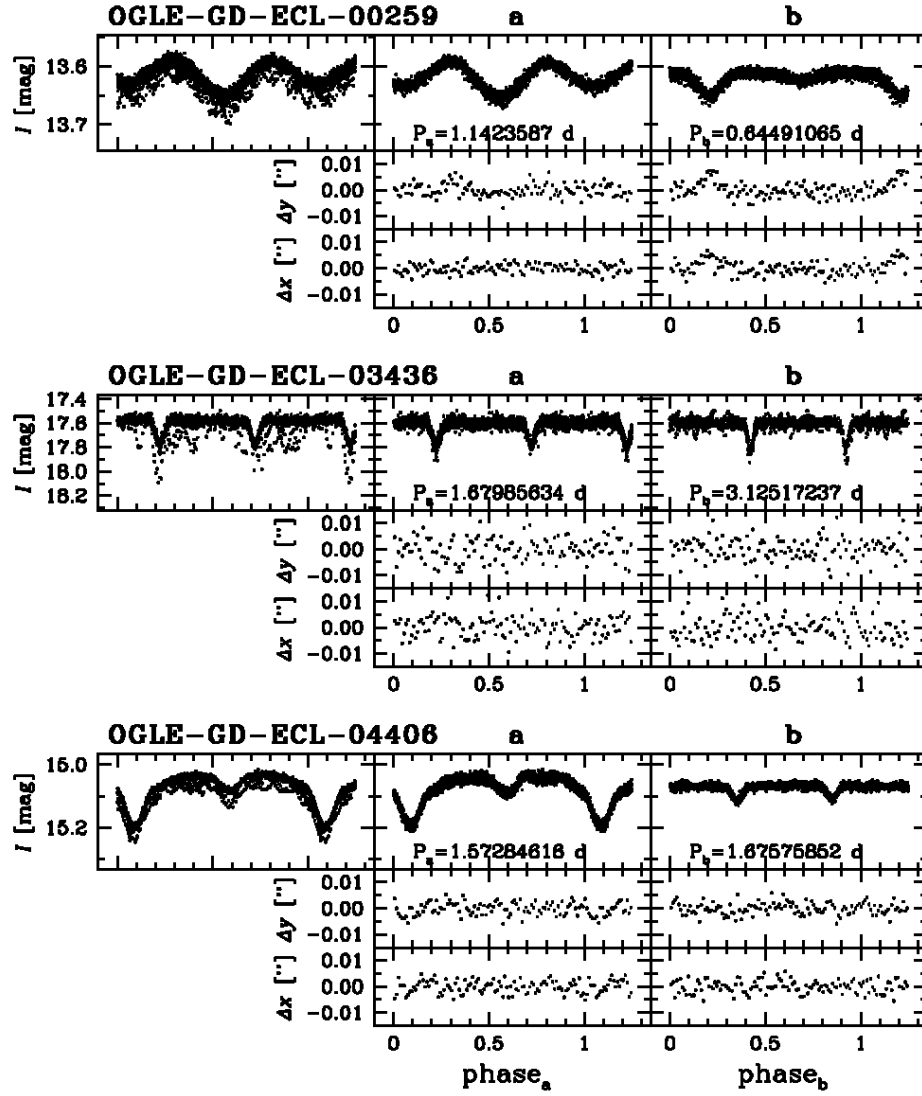


Fig. 7. Phased light curves of double binaries (left panels). Each component light curve ('a' and 'b', middle and right panels, respectively) is phased with the given period (P_a and P_b). The panels below the light curves show offsets in the position of centroids in the x and y directions of the CCD detector phased with the same periods. Clear correlation is seen in OGLE-GD-ECL-00259b between the phased light curve and offsets from the mean position in both directions and indicates high probability of chance alignment of the ellipsoidal binary OGLE-GD-ECL-00259a and the eclipsing binary OGLE-GD-ECL-00259b in the sky. A similar correlation occurs for component 'a' of OGLE-GD-ECL-04406. In the case of OGLE-GD-ECL-03436 no such clear correlation is seen, rising the probability of a physical relation between the two binaries.

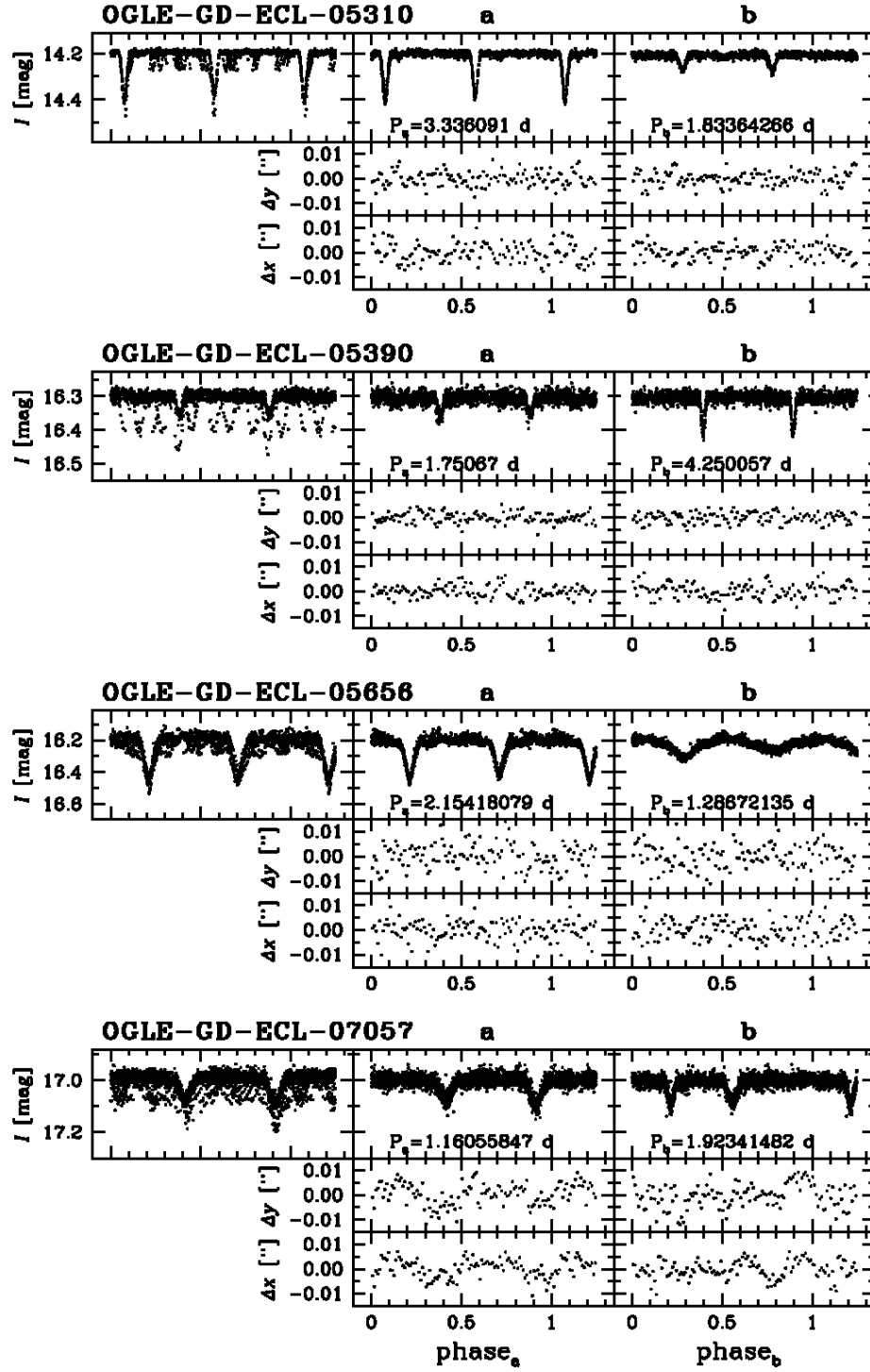


Fig. 8. Phased light curves of double binaries: OGLE-GD-ECL-05310, OGLE-GD-ECL-05390, OGLE-GD-ECL-05656, OGLE-GD-ECL-07057. All four doubly eclipsing binaries are likely quadruple systems.

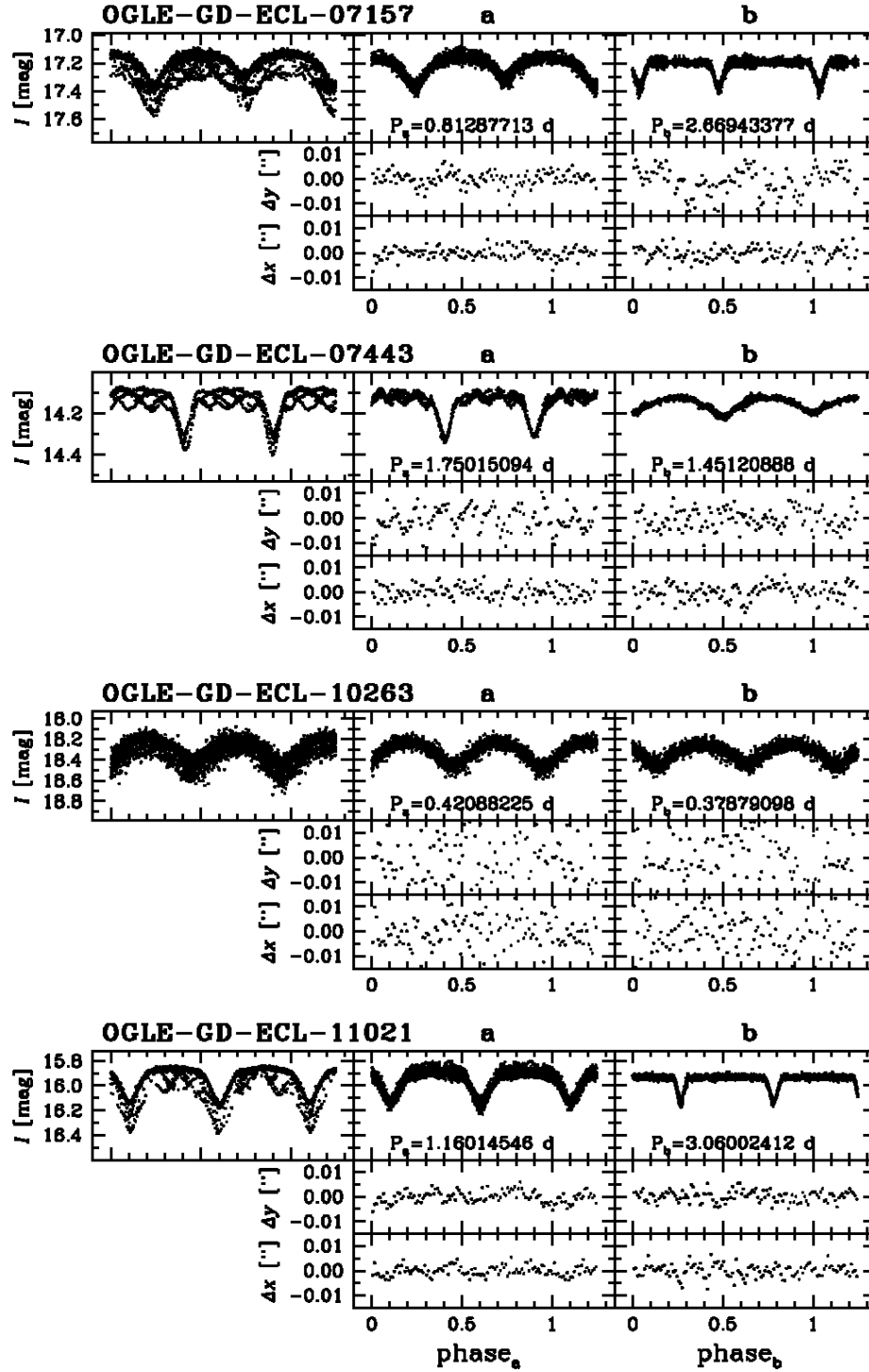


Fig. 9. Phased light curves of double binaries: OGLE-GD-ECL-07157, OGLE-GD-ECL-07443, OGLE-GD-ECL-10263, OGLE-GD-ECL-11021. All four doubly eclipsing binaries are likely quadruple systems. In the light curve of OGLE-GD-ECL-07443a, one can notice additional variations. After subtraction of the main signal with $P_a = 1.75015094$ d we obtained a modulation with a period of 0.290005 d, probably due to spots on the surface of one of the stars.

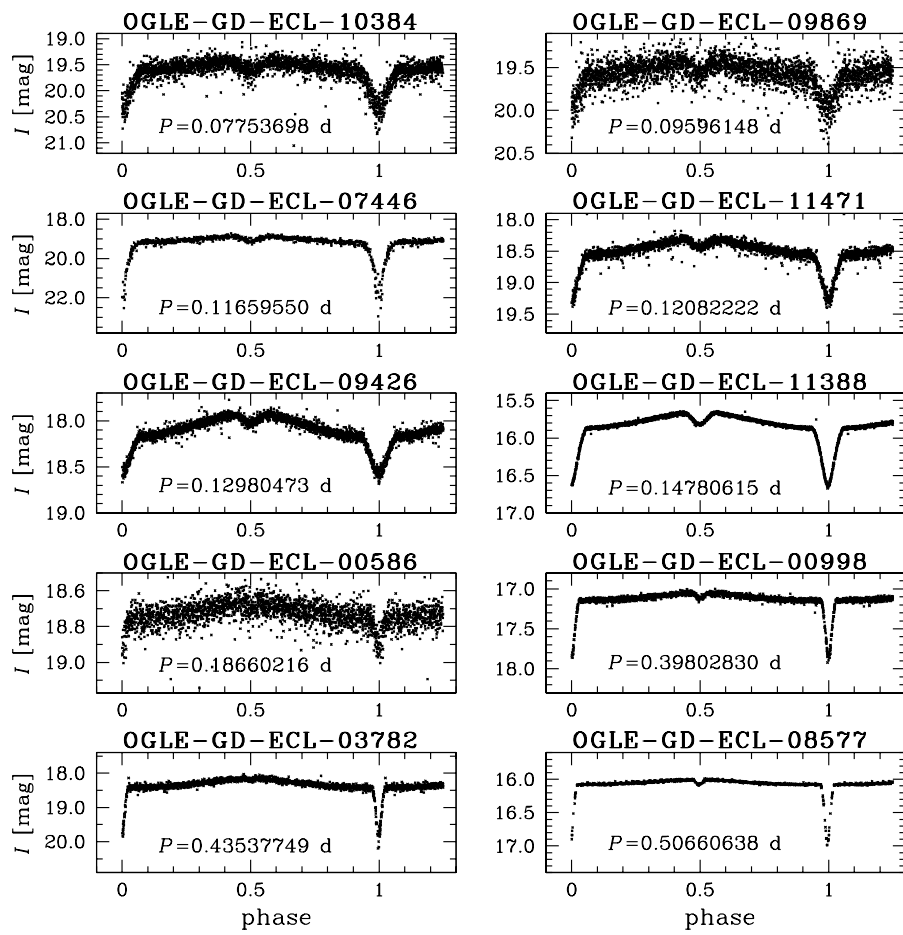


Fig. 10. Light curves of ten newly discovered sdB type binaries arranged with the increasing orbital period.

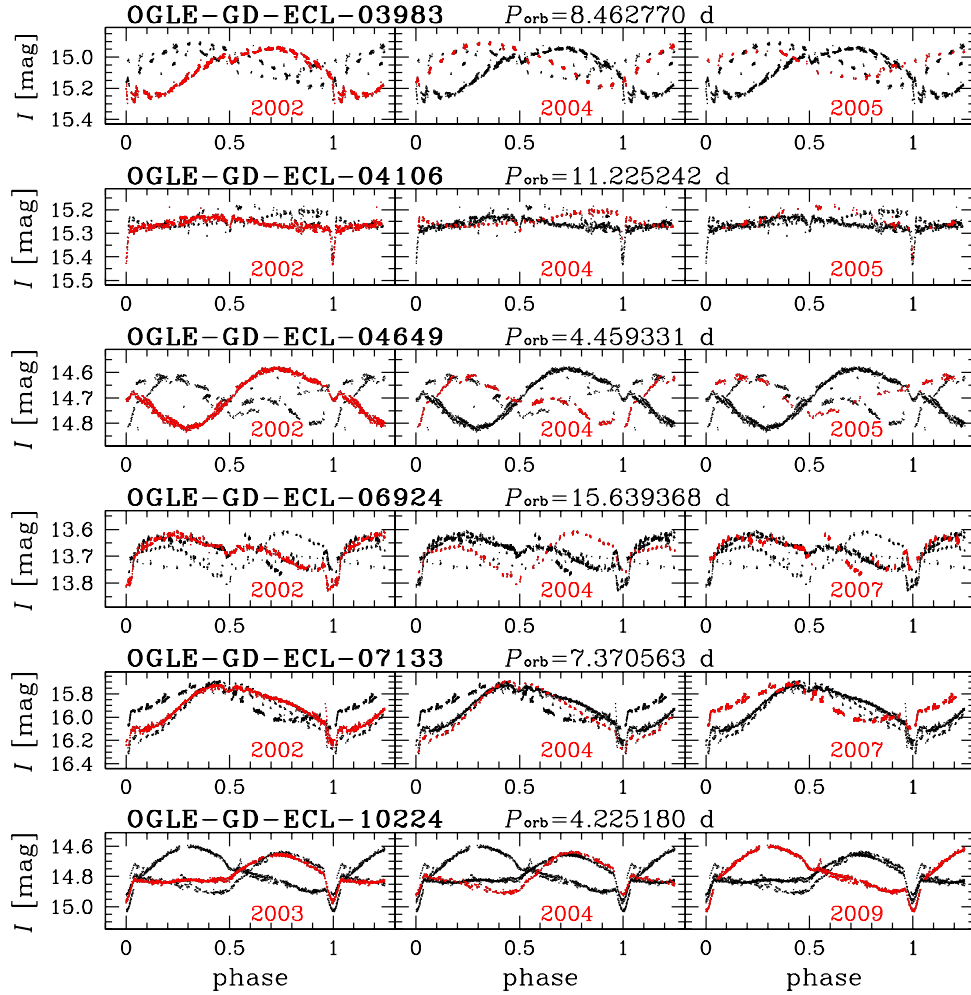


Fig. 11. Example light curves of six eclipsing RS CVn type stars identified in the OGLE-III disk area. The light curves are phased with the given orbital period. The changing starspot wave is highlighted in red for three best-covered seasons. Variable OGLE-GD-ECL-04649 shows both a single and a double starspot wave at various seasons, indicating the presence of two dark spot regions on opposite hemispheres.

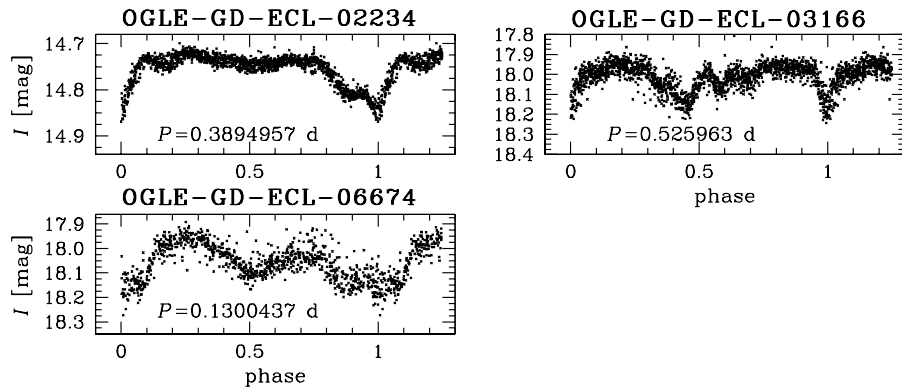


Fig. 12. Phased light curves of three eclipsing objects of unknown nature.

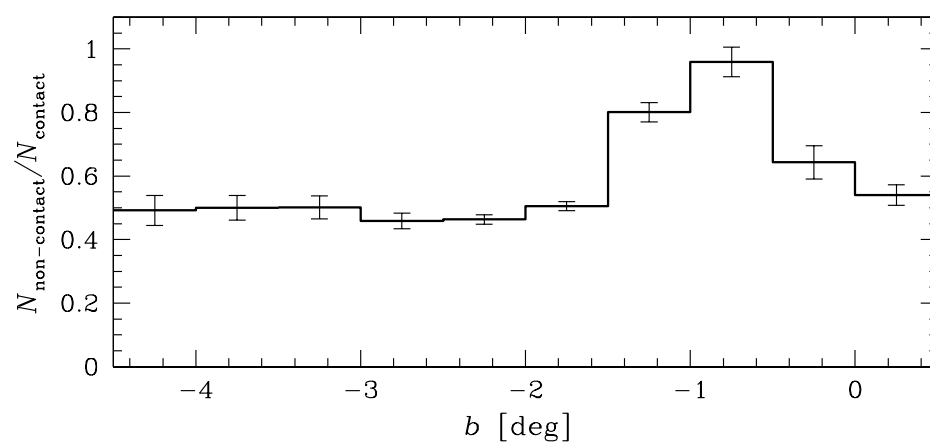


Fig. 13. Noncontact-to-contact binary ratio as a function of the Galactic latitude. Note a significant increase of the ratio around latitude -1° .